[CANCER RESEARCH 61, 4994–5001, July 1, 2001]

Runt-related Gene 2 in Endothelial Cells: Inducible Expression and Specific Regulation of Cell Migration and Invasion[1]

Lixin Sun, Michele Vitolo, and Antonino Passaniti[2]

Departments of Pathology [L. S., A. P.] and Biochemistry and Molecular Biology [M. V., A. P.], and the Greenebaum Cancer Center Program in Oncology and Experimental Therapeutics [L. S., A. P.], University of Maryland School of Medicine, Baltimore, Maryland 21201

ABSTRACT

Understanding the regulation of endothelial cell (EC) gene expression has important implications for angiogenesis, tumor growth, and metastasis. The transcription factor runt-related gene 2 (RUNX2)/core binding factorα-1/acute myeloid leukemia 3/polyoma enhancer-binding protein 2αA/osteoblast-specific transcription factor 2 regulates osteoblast differentiation, increases lymphomagenesis in transgenic mice, and is expressed in murine ECs. Here, we report on RUNX2 expression in human bone marrow EC (HBME-1) and its role in EC differentiation. Expression of RUNX2 occurred in HBME-1 cultured on extracellular matrix (ECM) substrates that stimulate *in vitro* differentiation (tube formation). Neutralizing anti-insulin-like growth factor (IGF)-I-receptor antibody inhibited tube formation as well as activation of RUNX2 expression in HBME-1 cultured on ECM. IGF-I treatment also increased both RUNX2 mRNA and protein expression. HBME-1 transfectants expressing dominant-negative (DN) RUNX were established to address the role of RUNX2 in these processes. HBME/DN cells exhibited reduced tube formation activity relative to control transfectants and less ability to growth arrest and differentiate on ECM. DNRUNX expression also inhibited HBME-1 migration and invasion, which are necessary for tube formation. The urokinase-type plasminogen activator and membrane-type MMP-1 genes were consistently down-regulated in DNRUNX transfectants. The results suggest that RUNX2 is important in IGF-I and ECM-regulated EC migration and differentiation. RUNX2 effects on HBME-1 migration and invasion may occur through activation of protease expression, events that regulate angiogenesis, and tumor growth.

INTRODUCTION

The sprouting and maturation of new blood vessels, or angiogenesis, provides nutrients and oxygen for solid tumor growth and is more likely to result in metastatic disease (1–3). Angiogenesis is also activated in the bone marrow in hematopoietic malignancies such as AML,[3] chronic myeloid leukemia, acute lymphocytic leukemia, and chronic lymphocytic leukemia (4–7). Therefore, an understanding of the events necessary for angiogenesis may facilitate both the screening of potential therapeutic agents and the development of targeting strategies in cancer treatment.

Vessel sprouting and maturation depends on EC activation, a process regulated by complex molecular interactions involving proangiogenic factors, proinflammatory cytokines, hemostatic factors, and components of the ECM (8–11). As the EC is activated from a normally quiescent state, it undergoes proliferation, migration, differentiation, and synthesis of proteases such as uPAs and MMPs (12, 13). These proteases catalyze the digestion of the ECM and enable ECs to invade and migrate. They also promote EC survival and influence matrix remodeling during vessel maturation (14). The transcriptional induction of these genes in activated ECs is a critical and early event necessary for angiogenesis. For example, expression of the Ets-1 transcription factor after vascular endothelial growth factor and fibroblast growth factor-2 treatment regulates the transcription of uPA, MMP1, MMP3, and MMP9 (15, 16), whereas reduction of Ets-1 impairs EC migration and invasion (17, 18). Knockout mice in the Id genes exhibit vascular malformations and fail to adequately vascularize implanted tumors, leading to extensive necrosis (19). MEF-2C null mice exhibit impaired cardiogenesis and reduced expression of angiopoietin-1 and vascular endothelial growth factor (20). Although expression of some of the transcription factors involved in angiogenesis, such as TAL-1 and Vezf, appears to be restricted to ECs (21, 22), others, such as fos/jun (23), nuclear factor κB (24), estrogen receptor (25), cAMP-responsive element binding protein (26), and hypoxia inducible factor-1 (27) are expressed by vascular and nonvascular cells.

The RUNX2/Cbfα1/AML3/polyoma enhancer-binding protein 2αA/osteoblast-specific transcription factor 2 is a member of the mammalian RUNX family, which also includes RUNX1/Cbfα2/AML1 and RUNX3/Cbfα3/AML2. The RUNXs bind DNA through a conserved Runt-homology domain and form a heterodimer with Cbfβ (28). The RUNXs are all involved in hematopoiesis (28). The RUNX1 knockout mice died of hemorrhage (29), and the embryos showed impaired angiogenesis because of dysfunction of hematopoietic stem cells (30). Although RUNX2 was originally thought to be a T-cell-specific gene (28), its essential function in skeletal development (osteogenesis and chondrogenesis) has been clearly defined (31–33). RUNX1 and RUNX2 were shown recently to be up-regulated by angiogenic cytokines in a murine EC model and may regulate expression of the angiopoietin-1 gene (34). However, expression of RUNX2 in human ECs, its role in regulating EC migration and invasion, and what other target genes may be activated by RUNX2 have not been clearly defined.

In the current study, induction of RUNX2 expression in a HBME-1 line by ECM and IGF-1 was examined. The specific effect of RUNX2 on EC migration and protease expression was studied by introducing a DNRUNX to block its transcriptional activity in HBME-1.

MATERIALS AND METHODS

Reagents

AML3 (RUNX2)-specific antibody was obtained from Oncogene Research Products (Cambridge, MA). IGF-1 and anti-γ-tubulin antibody were from Sigma Chemical Co. (St. Louis, MO). Neutralizing antibodies for β1-integrin and IGF-1 receptor were obtained from Life Technologies, Inc. (Rockville, MD) and R&D Systems (Minneapolis, MN), respectively. Rat-tail collagen (collagen type I) was from BD Biosciences (San Jose, CA). Matrigel (EHS

Received 11/20/00; accepted 4/27/01.

The costs of publication of this article were defrayed in part by the payment of page charges. This article must therefore be hereby marked *advertisement* in accordance with 18 U.S.C. Section 1734 solely to indicate this fact.

[1] Supported by University of Maryland Greenebaum Cancer Center Funds (to A. P., L. S.) and by a Predoctoral Training Grant from the Combined Doctoral Program in Biochemistry, Department of Biochemistry and Molecular Biology (to M. V.).

[2] To whom requests for reprints should be addressed, at University of Maryland Greenebaum Cancer Center, BRB Room 7-021, 655 West Baltimore Street, Baltimore, MD 21201. Phone: (410) 328-5470; Fax: (410) 328-6559; E-mail: apass001@umaryland.edu.

[3] The abbreviations used are: AML, acute myeloid leukemia; RUNX, Runt-related gene; EC, endothelial cell; ECM, extracellular matrix; Matrigel, Englebreth-Holm-Swarm matrix; DN, dominant negative; IGF, insulin-like growth factor-1; Baec, bovine aortic EC; Cbf, core binding factor; Huvec, human umbilical vein ECs; HBME-1, human bone marrow EC; Ang1, angiopoietin-1; HMEC, human dermal microvasculature EC; PEBP2, polyomavirus enhancer binding protein-2; Osf2, osteoblast-specific factor-2; uPA, urokinase-type plasminogen activator; MT1, membrane type 1; Tie2, angiopoietin receptor; MMP, matrix metalloproteinase; OPN, osteopontin; GAPDH, glyceraldehyde-3-phosphate dehydrogenase; RT-PCR, reverse-transcription PCR; TCA, trichloroacetic acid; CSS, charcoal-stripped serum.

matrix) was prepared in the laboratory from the EHS tumor as described (35) and used at a protein concentration of 8–10 mg/ml

Cell Cultures

HBME-1 cells (36), a gift from Dr. Kenneth Pienta (University of Michigan, Ann Arbor Comprehensive Cancer Center, Michigan) and Baec, purchased from the Coriell Cell Repository (Camden, NJ), were maintained in DMEM containing 10% FBS and antibiotics (Penicillin, Streptomycin, and Amphotericin B) from Life Technologies, Inc. Huvec were purchased from Clonetics (Walkersville, MD), and HMEC-1 (37) were obtained from Dr. Francisco Candal (Centers for Disease Control and Prevention, Atlanta, GA). Huvec and HMEC-1 were cultured in Medium 199 (Biofluid, Rockville, MD) containing 10% FBS, bovine brain extract (3 μg/ml), epidermal growth factor (10 ng/ml), hydrocortisone (1 μg/ml), and antibiotics (Penicillin/Streptomycin/Amphotericin B). Huvec and Baec cells were used at passage 8 or less. HMEC-1 was used between passage 8 and 14. HBME-1 was used between passage 14 and 24.

Plasmid Preparation

RT-PCR subcloning was used to construct a DNRUNX expression plasmid (pcDNA3-DNRUNX). The RT-PCR product of DNRUNX amplified from HBME-1 total RNA by RUNX2-specific primers (5′GGAATTCACCATGGTGGAGATCATCG; 5′GGGATCCTTCAAAGCTTCTGTCTGTG) was inserted into the pGEM-T vector (Promega, Madison, WI) and sequenced. DNRUNX insert was religated with the pcDNA3.0 (−) expression vector (Invitrogen, Carlsbad, CA). A reporter plasmid pGL3-Ose2-Luc was constructed by inserting 2 repeats of the consensus RUNX binding site (Ose2; Ref. 32) in the pGL3-min vector (Promega). The double-strand insert was generated from the following oligonucleotides with RUNX binding sites underlined and cohesive ends in bold:

5′-**AGCTT**GCAATCACCAACCACAGCAGCAATCACCAACCACA-GC**A**-3′

3′-**AC**GTTAGTGGTTGGTGTCGTCGTTAGTGGTTGGTGTCG**TTCG-A**-5′

Stable Transfection

Transfection of HBME-1 with pcDNA-DNRUNX and pcDNA3.0 vector was carried out with Superfect transfection reagent according to the protocol provided by the manufacturer (Qiagen Inc., Valencia, CA). Two days after transfection, stable transfectants were selected with 0.8 mg/ml of geneticin (Life Technologies, Inc.) for 2 weeks. To confirm the expression of DNRUNX, RT-PCR was performed with T7 and bovine growth hormone reverse primers (Invitrogen).

EC Functional Assays

For these assays, confluent HBME-1 cells were starved in DMEM containing 0.1% BSA for 14 h before each experiment. Trypan blue exclusion was used to routinely monitor the cell viability. Matrigel-coated plates were prepared by applying ice-cold liquid Matrigel on the wells evenly and then incubating at 37°C for 30 min.

Differentiation Assays. Starved cells (1×10^6) were washed in serum-free DMEM and plated in a six-well plate with or without Matrigel coating (0.4 ml/well). Cells cultured on Matrigel were treated with or without neutralizing antibody to IGF-1 receptor or β1 integrin. Tube-like network formation was digitally photographed at different times using a Zeiss microscope equipped with computerized image analysis, and RNA was isolated for RUNX2 expression analysis by Northern blot.

Thymidine Incorporation. Five $\times 10^4$, 1.5×10^5, or 4.5×10^5 cells/well were cultured overnight in 0.5% FBS in 24-well uncoated plates or plates coated with Matrigel. After removing the medium, the cells were incubated with [^{3}H]thymidine (Amersham Pharmacia Biotech, Buckinghamshire, England) for 4 h (1 μCi/well) and were then fixed and permeabilized with cold 10% trichloroacetic acid for 10 min, rinsed with PBS, and extracted with 0.1 N NaOH. An equal volume of 0.1 N HCl was added to the cell extract, and the total volume (0.5 ml) was placed in liquid scintillation vials containing 4.5 ml of BioSafe scintillation mixture and counted in a Beckman LS5801 Scintillation Counter (Beckman/Coulter Inc., Somerset, NJ).

Gel Degradation Assays. Cell invasion through collagen gels was determined in six-well plates coated with 1.5 ml of collagen I (3 mg/ml). Liquid rat-tail collagen (4.4 mg/ml) in 0.01 N acetic acid was neutralized with equimolar NaOH and buffered with HEPES buffer (pH 7.4) from a 1 M stock for a final concentration of 25 mM. DMEM was used to dilute the collagen to a final 3.0 mg/ml. All of the procedures were performed at 4°C. Cold collagen was poured into individual wells and allowed to gel at 37°C for 30 min prior to the addition of 5×10^5 cells/well in DMEM containing 0.5% FBS. After 16 h, invasive cells were photographed below the collagen layer.

Migration and Invasion Assays. Modified Boyden chamber assays as described previously (38) were used to determine cell migration and invasion activities. Briefly, Nucleopore filters (8-μm pore size) were coated with 0.1% neutralized type I collagen containing 1 μg/ml fibronectin (BD Biosciences, San Jose, CA) and placed on top of the lower chambers, which contained assay medium (0.1% BSA in DMEM) with attractants. Cells (2×10^5) in assay medium were added to the upper chamber. After 16-h incubation at 37°C under 5% CO_2, the filters were fixed with 3.7% formaldehyde in PBS for 20 min and stained with 0.5% crystal violet in 25% methanol for 60 min. Nonmigrating cells on the top of the filters were removed with a cotton swab, the migrating cells on the lower surface of the membrane were extracted, and their absorbance at 595 nm was measured. For invasion experiments, the filters were coated with 5–250 μg of Matrigel after the collagen-coated layer was air-dried. The cells were added on top of the dried matrix, and the number of migrating cells on the bottom side of the filter was determined after 16-h incubation at 37°C.

RT-PCR. RT-PCR was performed as described previously (39). Briefly, total RNA was isolated with RNEasy columns (Qiagen, Chatsworth, VA) from different ECs. Reverse-transcribed cDNA synthesis was primed with oligo-dT using first-strand beads (Pharmacia, Piscataway, NJ). Reverse-transcribed cDNA synthesized from 100 ng of total RNA was amplified by PCR reaction with Taq polymerase (Promega) and gene-specific primers (see Table 1). The BLASTN program (National Center for Biotechnology Information, Bethesda, MD) was used to ensure that all of the primers were unique without homology to other mRNAs in the database.

Northern Blots. Confluent HBME-1 cells were starved in DMEM containing 0.1% BSA for 14 h before culture on Matrigel or treatment with IGF-1. Total cellular RNA was isolated with TRIzol reagent (Life Technologies, Inc.) and fractionated on a 1% formaldehyde agarose gel before transfer to a Hybond N^+-membrane (Amersham Pharmacia Biotech). The RUNX2 probe was prepared by releasing insert from pGEM-T plasmid (described above) and labeling with α-^{32}P-dATP (Amersham Pharmacia Biotech, NJ) using the random prime DNA-labeling system (Life Technologies, Inc.). After a 1-h prehybridization, hybridization was performed with the ^{32}P-labeled probe at 42°C for 18 h. The membrane was washed with 2 × SSC once at room temperature and with 0.1 × SSC twice at 42°C for 15 min. The membranes were exposed to Kodak XAR film overnight at −70°C.

Table 1 *Primers used in PCR reaction*

Gene	Sequences	GenBank accession no.[a]	Product
RUNX2[b]	5′-GCACAGACAGAAGCTTGAT 5′-CCCAGTTCTGAAGCACCT	XM_004126	416 bp
uPA	5′-CCGGACTATACAGACCATCT 5′-AGTGTGAGACTCTCGTGTAG	A18397	367 bp
MT1-MMP	5′-GCATTGGGTGTTTGATGAGG 5′-GTTCTACCTTCAGCTTCTGG	D26512	327 bp
MMP2	5′-GCTGGAGACAAATTCTGG 5′-ACGACGGCATCCAGGTTAT	NM_008610	113 bp
Ang1	5′-GGGGGAGGTTGGACTGTAAT 5′-AGGGCATTTGCACATACA	U83508	362 bp
Tie2	5′-ATCCCATTTGCAAAGCTTCTGGCTGGC 5′-TGTGAAGCGTCTCACAGGTCCAGGAG	L06139	511 bp
OPN	5′-CGTGAATTCCACAGCCATGA 5′-CATAGACATAACCCTGAAGC	Gpaf05124	350 bp
GAPDH	5′-GATCCCTCCAAAATCAAGTG 5′-GACGCCTGCTTCACCACCTT	X01677	548 bp
CP[c]	5′-CATCCTGAAGCATACAGGTC 5′-CAGAAGGAATGGTTTGATGG	M19533.1	276 bp

[a] Primers were designed based on the sequences in the GenBank.
[b] RUNX2 primers amplify the RUNX2 from 645 bp to 1061 bp and therefore did not distinguish RUNX2 isoforms that are different in their NH_2-terminal sequences.
[c] CP, cyclophilin.

Luciferase Assays. HBME-1 parental cells and transfectants were plated in 12-well plates at an initial density of 4×10^5 cells/well in complete medium the day before transfection. The cells were transfected with 1 μg of the reporter plasmid pGL3–2XOse2-Luc or control vector pGL3-min using lipofectin reagent (Life Technologies, Inc.). In each case, 12.5 ng of pRL-Luc was cotransfected to provide a means of normalizing the assays for transfection efficiency. After transfection, the cells were washed with PBS and incubated in DMEM containing 0.5% FBS for 48 h. The luciferase activities derived from reporter and control plasmids were measured separately with the Dual-Luciferase Reporter assay system using a Turner Systems dual-wavelength luminometer and the protocol suggested by the manufacturer (Promega).

Protein Immunoblotting. Whole cell extracts were prepared as described (40). Cells were rinsed with PBS containing protease inhibitor mixture (Complete, mini-mixture tablets; Roche Diagnostics, Mannheim, Germany) and then harvested in 1 × SDS-PAGE loading buffer (2% SDS, 2 M urea, 10 mM DTT, 10% glycerol, 10 mM Tris-HCl, 0.0002% bromphenol blue, and 1.0 mM phenylmethylsulfonyl fluoride). Huvec, HMEC-1, Baec, and HBME-1 were cultured on plastic plate in complete medium. HBME-1 cells were starved in DMEM containing 0.1% BSA for 14 h before IGF-1 treatment. To compensate for the increased cell numbers in cytokine-treated samples, aliquots of whole cell extracts equivalent to 10 μg of DNA were run on 10% SDS-PAGE gels and electrotransferred to nitrocellulose membranes (Novex, San Diego, CA). The blots were incubated with anti-RUNX2-specific antibody at a 1:400 dilution followed by horseradish peroxidase-conjugated goat antirabbit IgG (KPL, Gaithersburg, MD) and detected by enhanced chemiluminescence (Amersham Pharmacia Biotech). γ-Tubulin was used as a loading control and was measured by reprobing the stripped membrane with anti-γ-tubulin antibody (Sigma Chemical Co.).

Statistical Analyses. The NIH Image Analysis program was used to calculate relative densities of RT-PCR products, Northern blots, or Western blots. The Statview program and Student's *t* test were used to determine significance values.

RESULTS

Expression of RUNX2 in Human and Bovine ECs. To evaluate the involvement of RUNX2 in angiogenesis, the expression of RUNX2 in human and bovine EC was examined by RT-PCR and Western blot. RUNX2 mRNA and protein were present in all of the cells examined including primary ECs (Huvec and Baec) and T-antigen immortalized EC lines (HBME-1 and HMEC-1; Fig. 1*A*). The levels of RUNX2 mRNA and protein in most of these ECs, except for the HBME-1, were quite low. As measured relative to GAPDH or γ-tubulin, 5.7-fold more mRNA and 2.6-fold more protein was detected in HBME-1 cells than in Huvec cells, respectively. Serum withdrawal resulted in rapid diminution of RUNX2 message in HBME-1 cells with a half-life of 3 h (Fig. 1, *B* and *C*).

Induction of RUNX2 Expression in HBME-1 Cultured on ECM or Treated with IGF-1. EC tube formation on ECM is a commonly used *in vitro* model of differentiation and angiogenesis. To examine whether RUNX2 expression is activated during EC differentiation, serum-starved HBME-1 cells were cultured on ECM (Matrigel) to induce tube formation, and RUNX2 expression was measured in the differentiating cells by Northern blots. Cells on plastic formed a monolayer (Fig. 2*A*, *PL*) and expressed low RUNX2 message (Fig. 2*B*, *PL*). Cultured on ECM (Matrigel), HBME-1 formed tube-like structures (Fig. 2*A*, *MG-1*), which corresponded to a dramatic elevation of RUNX2 expression. (Fig. 2*B*, *MG-1*). IGF-1 has been shown to be an important component of matrix and an angiogenic factor (41), which also stimulates EC differentiation (tube formation) *in vitro* (42). Like many bone-derived cells, HBME-1 cells express IGF-1 receptor (not shown). To examine whether cell-matrix interactions and IGF-1 were involved in the regulation of RUNX2 expression and EC tube formation, neutralizing antibodies to IGF-1 receptor and β1-integrin were used. Compared with anti-β-catenin control-antibody treatment (not shown), treatment with β1-integrin antibody (1:100), which mediates EC adhesion and migration, completely abolished tube formation (Fig. 2*A*, *MG-2*). However, it did not affect elevation of RUNX2 by ECM (Fig. 2*B*, *MG-2*). Neutralizing IGF-1-receptor antibody (1:400 dilution) inhibited tube formation (Fig. 2*A*, *MG-3*) and induction of RUNX2 by ECM (Fig. 2*B*, *MG-3*). Relative to plastic, ECM induction of RUNX2 was 9-fold, 10.5-fold, and 5.7-fold in ECM only, ECM + integrin antibody, and ECM + IGF-1-receptor antibody respectively. In the absence of Matrigel, IGF-1 treatment stimulated RUNX2 expression in a dose-dependent manner as determined by Northern blotting (Fig. 3, *A* and *B*). A log scale was used to calculate an EC_{50} value of 14 pM (0.1 ng/ml). Western blot analysis showed that IGF-1 stimulated the expression of RUNX2 proteins 2.1-fold above controls after 3 h. A higher molecular weight form of RUNX2 protein was also observed after IGF-1 treatment (Fig. 3*C*).

Introduction of a DN Form of RUNX in HBME-1. Truncated RUNX2 cDNA encoding the DNA binding (Runt) domain acts as a DN inhibitor for RUNX (DNRUNX) in murine preosteoblast cells by

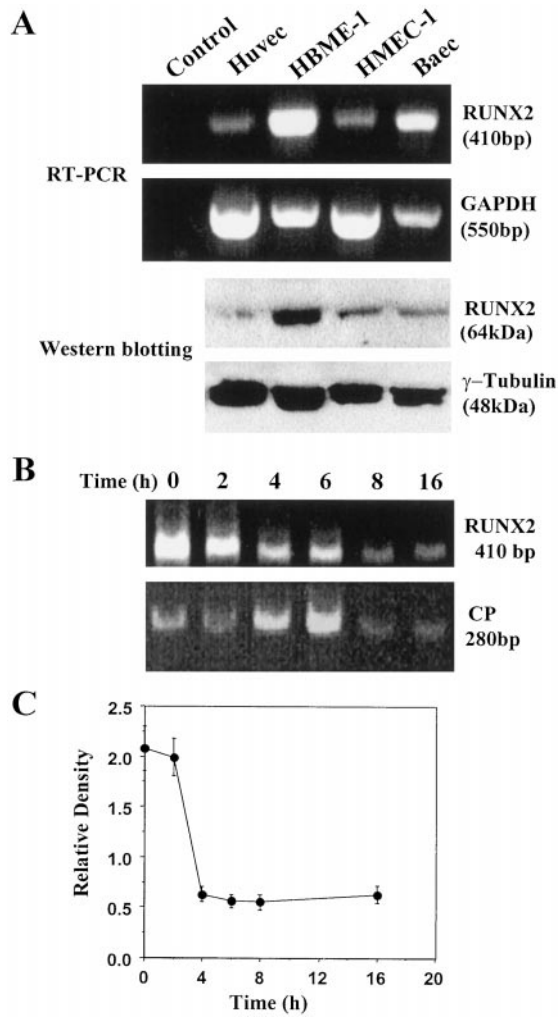

Fig. 1. *A*, expression of RUNX2 in ECs analyzed by RT-PCR and Western blotting. Huvec, HBME-1, HMEC-1, and Baec cells were cultured in complete medium. RNA and protein were isolated as described in "Materials and Methods." Note low RUNX2 expression in Huvec (primary umbilical vein EC) and HMEC-1 (dermal microvascular) relative to HBME-1 (bone marrow) cells. A negative control for the same PCR reaction in the absence of cDNA template is shown. RT-PCR reactions and Western blots are representative of three separate experiments. *B*, reduced RUNX2 expression in HBME-1 in the absence of serum. HBME-1 cells were incubated in the absence of FBS for 0–16 h and RNA was prepared. RUNX2 levels were examined by RT-PCR, and cyclophilin (*CP*) was used in the PCR reaction as an internal control. *C*, intensities of PCR products were measured by NIH Image software and represented as relative intensity of RUNX2 normalized to CP. The data are representative of three separate experiments; *bars*, SD.

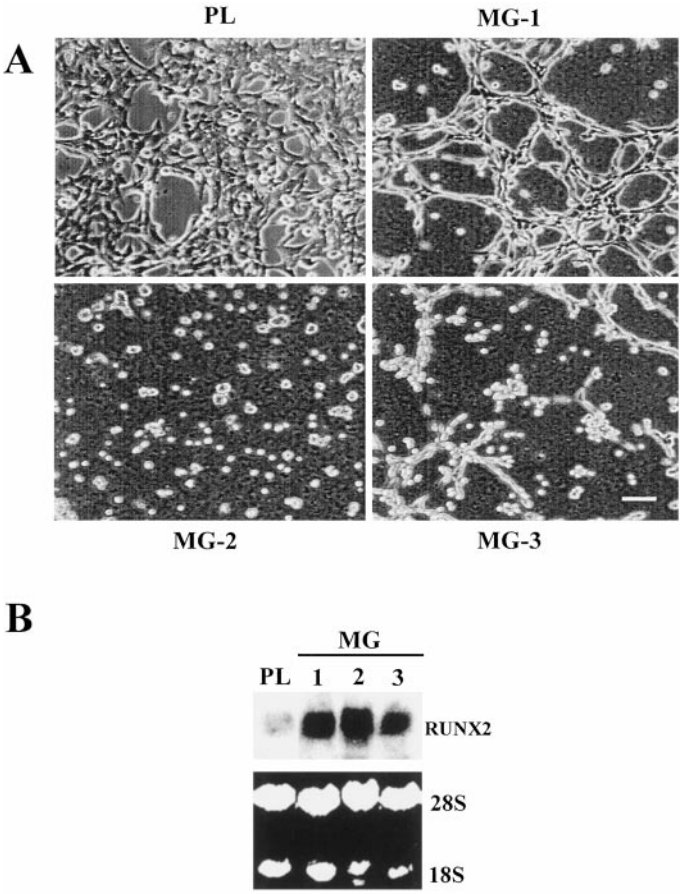

Fig. 2. Correlation of RUNX2 expression and morphological features of EC differentiation on ECM. *A*, HBME-1 tube formation on ECM (Matrigel). HBME-1 cells incubated in the absence of FBS for 14 h were harvested with trypsin/EDTA and transferred to six-well plate with or without Matrigel coating (*MG* or *PL*) in the absence of serum. HBME-1 cells formed a typical EC monolayer on plastic (*PL*) and organized into tubes on ECM (*MG-1*). Cells treated with neutralizing antibody to β1 integrin at 1:100 dilution (*MG-2*) or with anti-IGF-1 receptor antibody at 1:400 dilution (*MG-3*) showed reduced tube formation on ECM under the same conditions. *Bar*, 1 cm = 100 μm. *B*, Northern blot analysis of RUNX2 expression. RUNX2 expression corresponding to HBME-1 tube-formation (*A*) was analyzed by Northern blots. Equal total RNA (30 μg) from HBME-1 was applied per lane: PL, on plastic; MG-1, on ECM; MG-2, with anti-β1 antibody (1:100) on ECM; and MG-3, with anti-IGF-1-receptor antibody (1:400) on ECM. Equal loading was confirmed by 28 s/18 s rRNA stained with ethidium bromide. Data are representative of three separate experiments.

competing with RUNX for DNA binding and inhibiting their transcriptional activities (33). To clarify the roles of RUNX2 in endothelial tube formation, we established a stable DNRUNX transfectant of HBME cells (HBME/DN) by introducing the Runt domain cDNA into HBME-1 cells. For selection of stable DNRUNX transfectants, a pooled population of surviving cells was expanded and examined for expression of the DNRUNX construct. The expected 549-bp fragment was detected by RT-PCR in DNRUNX-transfected cells whereas control neotransfected cells (HBME/neo) expressed a 156-bp mRNA consistent with a lack of cloned insert (Fig. 4*A*). Sequence analysis of the 549-bp fragment confirmed the authenticity and orientation of the Runt domain (not shown). RUNX transcriptional activities in HBME-1 transfectants were assessed by transfection of a luciferase reporter gene driven by a 2 $\times$ consensus RUNX-binding site (Ose2) in the pGL3min vector (pGL3-Ose2-Luc). Both HBME-1 and HBME/neo cells exhibited increased luciferase activity when transfected with the pGL3-Ose2-Luc compared with pGL3min vector alone, whereas luciferase activity in HBME/DN cells did not increase significantly (Fig. 4*B*). Fold-induction of luciferase activity was 2.90 $\pm$ 0.90, 3.4 $\pm$ 0.27, and 1.28 $\pm$ 0.01 in HBME, HBME/neo, and HBME/DN cells, respectively. HBME/DN and HBME/neo expressed similar levels of IGF-1 receptor and responded to IGF-1 or Matrigel treatment with similar increases in endogenous levels of RUNX2 (not shown).

RUNX2 Regulates EC Differentiation and Migration. The HBME/DN cells were used to examine the function of RUNX2 in endothelial differentiation. Culture of HBME/neo cells on Matrigel in the absence of FBS for 3 h activated the initial morphological changes necessary for tube formation (Fig. 5*A*, *a*), but HBME/DN migration was delayed (Fig. 5*A*, *b*). After additional culture, both HBME/neo and HBME/DN cells were capable of tube formation (not shown). Culture of HBME/neo cells in 2% CSS for 16 h on plastic (Fig. 5*A*, *c*) also resulted in morphological changes indicative of tube formation. However, HBME/DN cells formed a monolayer, and their differentiation potential was severely compromised under the same conditions (Fig. 5*A*, *d*). Endothelial growth arrest is associated with differentiation and tube formation on ECM. The response of HBME/DN to matrix-induced growth arrest was analyzed by thymidine incorporation. At three different cell densities tested, HBME/neo

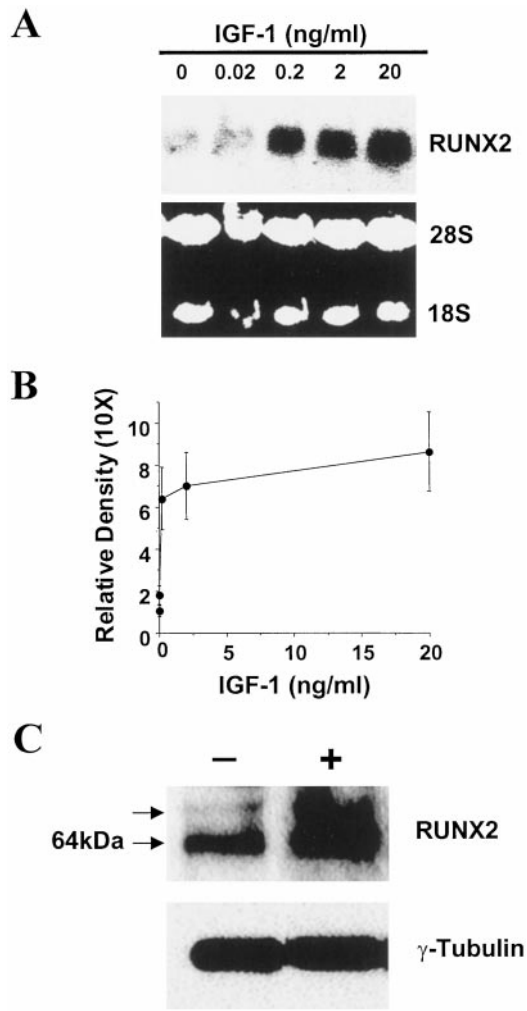

Fig. 3. *A* and *B*, IGF-1 induction of RUNX2: dose response analyzed by Northern blot. Cells were starved for 14 h prior to IGF-1 treatment. After 6-h treatment, total RNA was isolated, resolved on agarose gels, and probed with the RUNX2 probe. *B*, band intensities were calculated with the NIH Image software and are presented in arbitrary units relative to 28S RNA *versus* IGF-1 concentration. Similar results were obtained from three separate experiments; *bars*, SD. *C*, RUNX2 protein expression in response to IGF-1. +, HBME-1 cells were treated with IGF-1 (2 ng/ml) for 3 h after an overnight starvation period. –, control cells were untreated. Whole cell lysates were resolved on SDS-PAGE, and anti-RUNX2 antibody was used to detect RUNX2. The same blots were stripped and reprobed with anti-γ-tubulin antibody to verify equal loading. *Arrows*, M_r 64,000 RUNX2 band and a higher molecular weight form of RUNX2.

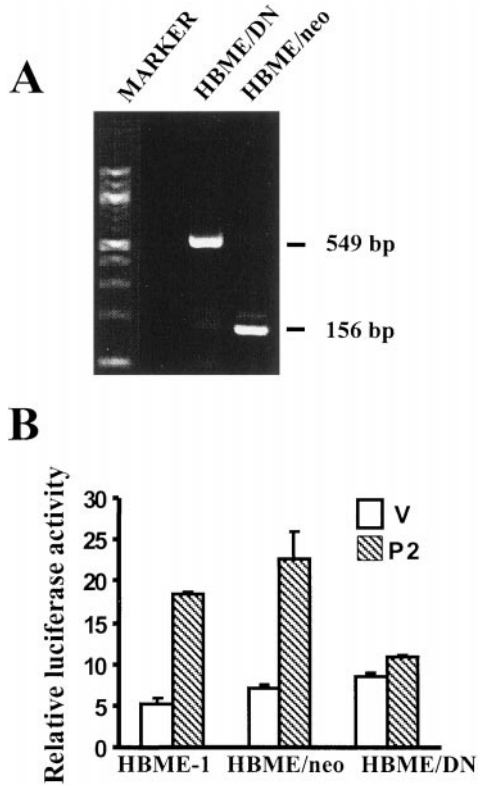

Fig. 4. *A*, characterization of DNRUNX transfectants: expression of DNRUNX in stable transfectants. RNA was isolated from HBME/DN or control HBME/neo transfectants. Primers flanking the DNRUNX insert in pcDNA3.0(−) plasmid were used in RT-PCR reactions. A 549-bp product was evident in HBME/DN and a 156-bp product lacking Runt insert (413 bp) was found in HBME/neo. *B*, transcriptional activity of RUNX2 in HBME/DN analyzed by luciferase reporter assay. The luciferase-fusion construct and transient transcription were described in "Materials and Methods." The cells were transfected with reporter-plasmid, pGL3–2Xose2-Luc (*P2*), or control vector, pGL3min (*V*). The pRL-luc was cotransfected as an internal control of transfection efficiency. Data are an average of luciferase activity normalized to pRL-luc obtained from three independent transfection experiments; *bars*, SD.

cells showed lower thymidine incorporation relative to plastic when exposed to matrix. The ratio (matrix:plastic) was <1.0 (ratio = 0.65 ± 0.12) for HBME/neo cells. Conversely, HBME/DN cells exhibited a ratio (matrix:plastic) = 1.5 ± 0.06 (Fig. 5*B*). A ratio (matrix:plastic) >1.0 indicates an inability to growth arrest on matrix.

Tube formation on ECM is dependent on EC migration and invasion. To directly compare the invasive ability of HBME/DN with HBME/neo, cells were cultured on collagen I gel-coated plates. After 16 h, the cells were photographed at the surface of the gel (Fig. 6*A*, *a* and *c*) or at the surface of the plastic below the gel (Fig. 6*A*, *b* and *d*). HBME/DN failed to migrate and invade through the gel and grew on the gel surface (Fig. 6*A*, *a* and *b*) whereas HBME/neo degraded the gel and attached to the underlying plastic (Fig. 6*A*, *c* and *d*). For quantitative assessment of the chemotactic and invasive activities of the cells, a modified Boyden chamber assay was used in the presence of serum as an attractant. In response to 0.1% FBS, HBME/neo cells exhibited a 2.5-fold increased chemotaxis activity relative to HBME/DN cells. This difference was reduced to 1.5-fold with 1.0% FBS (Fig. 6*B*). Matrix protein-coated filters were used to quantitatively analyze the invasive capacities of the transfectants. As expected, increasing amounts of matrix protein (Matrigel)-coating decreased cellular invasion in both HBME/neo and HBME/DN. However, the migration of both transfectants on filters coated with 50 μg of matrix appeared to be higher or similar to migration on filters coated with 2.0 μg of matrix (Fig. 6*C*). This may be a reflection of the ability of ECM to increase RUNX2 expression (Fig. 2*B*, *MG-1*) or a general activation of the cells. Although the reduction of invasion was not linear with the amount of matrix, HBME/DN exhibited lower invasive activity than the HBME/neo at each dose of matrix coating.

Effect of DNRUNX on Expression of Endothelial Migration-related Genes. Because RUNX2 is a transcription factor, we analyzed the expression of several endothelial migration-related genes in the HBME/DN and HBME/neo cells. These cells were cultured in complete medium and RNA was prepared. Using a semiquantitative RT-PCR analysis with specific primers (Table 1), the expression of MMP-2, MT1-MMP, uPA, Ang1, Tie2, and OPN in HBME/DN and HBME/neo was compared. Among the genes examined, MT1-MMP and uPA were consistently expressed at lower levels in the HBME/DN cells relative to HBME/neo (Fig. 7). MMP-2, Ang1, and Tie2 gene expression did not decrease with DNRUNX transfection. Expression of OPN, which is directly regulated by RUNX2 in osteoblasts, was also not affected by DNRUNX (Fig. 7). Osteocalcin was undetectable by RT-PCR in HBME cells (not shown).

DISCUSSION

RUNX2 expression in murine ECs during angiogenesis has been reported recently (34). However, little is known about the regulation of RUNX2 expression in human ECs by cell-matrix interactions or

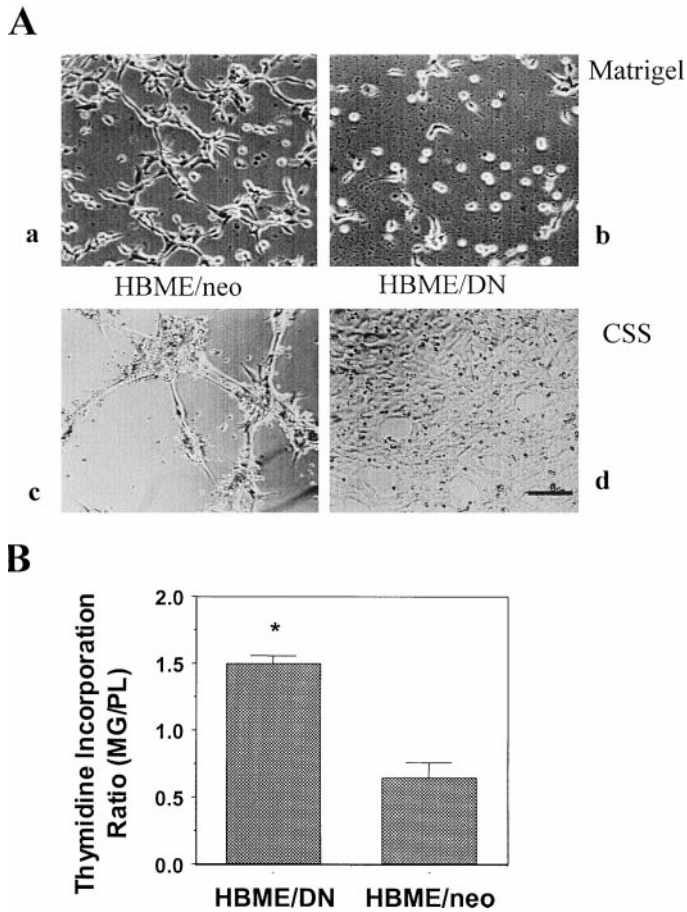

Fig. 5. *A*, effect of DNRUNX on HBME-1 differentiation: tube-formation. Initial tube formation activity of HBME/neo (*a* and *c*) or HBME/DN cells (*b* and *d*) on Matrigel (*a* and *b*) or on uncoated culture dishes in CSS (*c* and *d*). Cells (5×10^5) were cultured in six-well plates (*a* and *b*) for 3 h in the absence of serum. Cells (5×10^4) were cultured in 96-well plates (*c* and *d*) for 16 h in 2% CSS. *Bar*, 1 cm = 100 μm. *B*, thymidine incorporation ratio (Matrigel:plastic). Thymidine incorporation of HBME/neo and HBME/DN on plastic and on Matrigel was performed as described in "Materials and Methods." Data are presented as an average ratio of incorporation (Matrigel:plastic) from triplicate samples containing 50×10^3-450×10^3 cells; *bars*, SD. *, $P < 0.01$ *versus* HBME/neo.

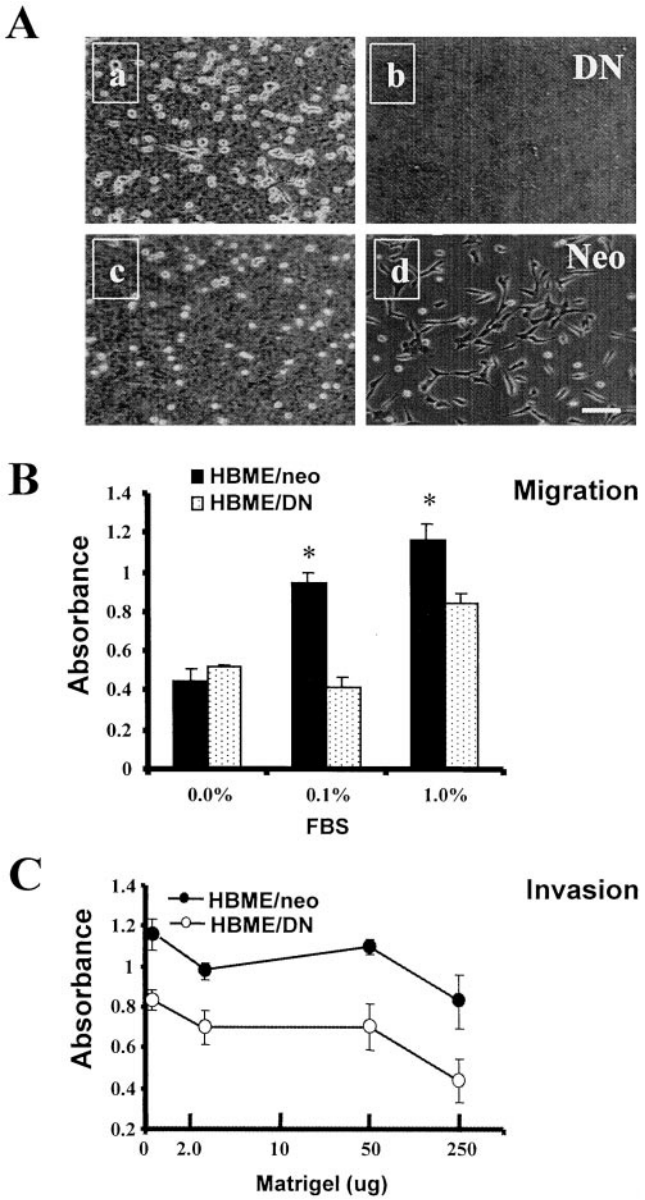

Fig. 6. *A*, effect of DNRUNX on EC invasion: degradation of collagen gel by HBME-1 cells. HBME/DN (*a* and *b*) and HBME/neo (*c* and *d*) were cultured on collagen I gels in a six-well plate (5×10^5 cells/well) for 16 h. Photographs were taken either at the surface of the gel (*a* and *c*) or at the surface of the plastic below the gel (*b* and *d*). Note that no HBME/DN cells migrated to the plastic (*b*). *Bar*, 1 cm = 100 μm. *B*, migration in modified Boyden chambers. HBME-1 cells (2×10^5/chamber) were cultured for 16 h on collagen-coated filters. Cell migration in response to FBS (0, 0.1, and 1.0%) in the bottom chamber was quantitated as described in "Materials and Methods." Results are representative of three different experiments and are the means of triplicate samples; *bars*, ± SD. *, $P < 0.01$ *versus* HBME/DN. *C*, invasion on Matrigel-coated filters. Except that Matrigel proteins (0–250 μg) were dried onto the filters prior to the addition of cells, the assay was performed as described above in the migration assays, and 1.0% FBS was used as attractant. Results from HBME/neo controls were significantly different from HBME/DN ($P < 0.01$) at each point.

IGF-1 treatment and the role of RUNX2 in EC invasion. Because ECs from different organs and different kinds of vessels (large and small vessels, veins, and arteries) display remarkable heterogeneity in gene expression profiles (43, 44), determination of RUNX2 expression in ECs isolated from different sources may provide important clues to its roles in angiogenesis. We report for the first time that RUNX2 is expressed in Huvec, HMEC-1, HBME-1, and Baec ECs. HBME-1 showed the most abundant expression among these cells in the presence of serum. This high-RUNX2 expression in HBME-1 was clearly not dependent on T-antigen expression because HMEC-1, which is derived from dermal microvasculature and immortalized with T antigen, expressed low levels of RUNX2. The bone marrow is the preferential site of metastasis for solid tumors of the prostate and breast (36, 45). In fact, previous findings showed that HBME-1 exhibits higher affinity for prostate tumor cells than Huvec (36). Bone marrow was reported to be the source of precursor ECs that can home to primary tumors to establish a neovasculature (42, 46). Survival of lymphoma and multiple myeloma cells may also depend on bone marrow ECs during tumor progression (47, 48). Therefore, use of HBME-1 cells to study RUNX2 function may be helpful to understand the role of angiogenesis in hematopoietic malignancies and tumor metastasis.

Exposure of HBME-1 to ECM resulted in the formation of tubule structures, which involves endothelial differentiation and migration (36). We found that RUNX2 expression in HBME-1 was dramatically elevated during this process. Because starved cells were used (low basal RUNX2 levels), the increase in RUNX2 expression is most likely attributable to transcriptional activation. Using a neutralizing antibody to IGF-1 receptor in the assay, tube formation and RUNX2 message induction were partially inhibited, suggesting that IGF-1 may be involved in RUNX2 induction by matrix. Indeed, IGF-1 treatment stimulated RUNX2 expression (EC_{50} value of 14 pM). IGF-1 is involved in bone metabolism (49) and is also an angiogenic factor (41, 42). The strong response of HBME-1 to IGF-1 is similar to the response of other bone marrow-derived cells, such as osteoblasts, to IGF-1. IGF-1 treatment also induced a higher molecular weight form of RUNX2 protein, which might result from RUNX2 phosphorylation. Previous reports have shown that RUNX2 activation is also mediated by protein phosphorylation. α2-Integrin in a murine preosteoblast cell line activated RUNX2 via phosphorylation of mitogen-activated protein kinase sites on RUNX2 without changes in mRNA

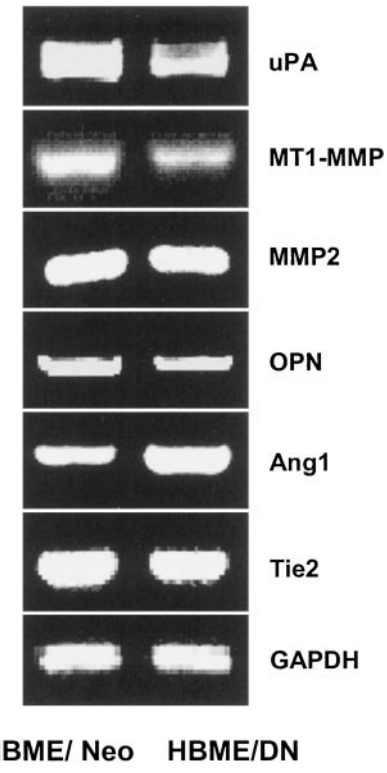

Fig. 7. Expression of migration and invasion-related genes in DNRUNX transfectants. Expression of uPA, MT1-MMP, MMP2, OPN, Ang1, and Tie-2 was compared between HBME/DN and HBME/neo by RT-PCR. GAPDH was used to normalize the template used in the PCR reactions. Shown is a representative example of three separate RT-PCR reactions with essentially similar results.

expression (40, 50). In our studies, β1-integrin neutralizing antibody did not inhibit RUNX2 mRNA expression whereas it blocked tube formation completely, indicating that β1-integrins may not regulate expression of RUNX2 in HBME-1. However, because β1-integrin interactions can stimulate mitogen-activated protein kinase (51), the possibility of β1-integrin activating RUNX2 through phosphorylation cannot be ruled out.

DNRUNX inhibit RUNX2-mediated chondrocyte differentiation (33) and murine EC tube formation (34). To address the role of RUNX2 in EC migration, invasion, and differentiation, which are required in the process of tube formation, a stable transfectant cell line (HBME/DN) was established by introducing the DNRUNX (human Runt cDNA) into HBME-1 cells. In studies characterizing the DNRUNX transfectant, we confirmed Runt domain was expressed in the stable HBME/DN transfectants but not the control HBME/neo cells. Moreover, the RUNX transcriptional activity was significantly reduced in HBME/DN compared with HBME/neo as assessed by a luciferase reporter containing consensus RUNX binding sites. The expression of IGF-1 receptor and the cell response to IGF-1 or ECM were not altered in these transfectants. HBME/DN cells exhibited a higher rate of DNA synthesis on matrix than HBME/neo. This is consistent with the reduced ability of HBME/DN to differentiate on ECM. Compared with HBME/neo, HBME/DN exhibited retarded migration on Matrigel, inability to degrade collagen I gel, and decreased chemotaxis and invasion capacity. Typically, an increase in the thickness of the matrix barrier will inhibit invasion (38). However, both transfectants showed increased invasive potential at intermediate doses of matrix proteins, suggesting that ECM (Matrigel)-degrading proteases may have been activated in HBME-1 after matrix binding.

Because the most dramatic effect of DNRUNX on HBME-1 was inhibition of cell migration and invasion, we examined the expression of several genes that are known to regulate these processes in EC. We did not see obvious decreases in MMP2, Ang-1, or Tie2 expression in the DNRUNX transfectants. OPN, a known downstream gene of RUNX2 in preosteoblasts (32), is also involved in EC migration by interaction with its receptor, $\alpha V\beta 3$, on ECs (52). However, its expression was not consistently inhibited in the HBME/DN cells. These results are similar to the observation in murine ECs (33), suggesting that RUNX2 regulation of OPN may require cooperation with other tissue-specific transcription factors. However, we found that uPA and MT1-MMP gene expressions were significantly down-regulated by DNRUNX transfection. uPA mediates a variety of biological functions and regulates EC adhesion, migration, and invasion (12). Likewise, MT1-MMP can directly degrade fibrin matrices and convert latent MMPs to active MMPs (53), which degrade ECM collagens. Plasmin generated by uPAs can also activate latent MMPs (54). Therefore, the inability of HBME/DN cells to invade through ECM and degrade collagen gels may result from inhibition of MMP activation. These results suggest a close correlation between RUNX2 function and activation of protease expression in ECs. The effects of DNRUNX on uPA and Ang-1 expression in our study differ from a previous report, which showed no change in uPA and decreased expression of Ang-1 in DNRUNX-transfected murine ECs (33). As mentioned above, these differences may result from EC heterogeneity and the nature of RUNX2, a tissue-specific transcription factor (55).

In conclusion, we have shown that several ECs from different tissues express RUNX2. In particular, HBME-1 exhibits abundant expression of RUNX2. Induction of RUNX2 expression in HBME-1 was correlated with tube formation activity after interaction with ECM. In addition, IGF-1 increased transcription of RUNX2 independently of matrix interactions. The specific effects of RUNX2 on EC invasion, migration, and differentiation were confirmed by introducing a DN form of RUNX into HBME-1. The decreased expression of uPA and MT1-MMP in HBME-1 after DNRUNX transfection suggests that RUNX2 may affect EC migration by up-regulating protease expression.

ACKNOWLEDGMENTS

We thank Dr. Kenneth Pienta (University of Michigan, Ann Arbor, Michigan) for generously providing the HBME cell line and Dr. Francisco Candal (Centers for Disease Control, Atlanta, GA) for the HMEC-1 cell line. We also thank Dr. Nicholas Ambulos for technical support and Lisa Sedgwick for oligonucleotide synthesis and sequencing (Biopolymer Unit, University of Maryland). Additionally, we thank Dr. Paul Shapiro (University of Maryland School of Pharmacy) for the generous gift of γ-tubulin antibody and Drs. Sanford Stass, Ann Hamburger, and Simeon Goldblum for their critical comments.

REFERENCES

1. Kerbel, R. S. Tumor angiogenesis: past, present, and the near future. Carcinogenesis (Lond.)., *21:* 505–515, 2000.
2. Klagsbrun, M. Angiogenesis and cancer: AACR special conference in cancer research. Cancer Res., *59:* 487–490, 1999.
3. Fidler, I. J. Angiogenesis and cancer metastasis. Cancer J. Sci. Am., *6* (Suppl. 2)*:* S134–141, 2000.
4. Perez-Atayde, A. R., Sallan, S. E., Tedrow, U., Connors, S., Allred, E., and Folkman, J. Spectrum of tumor angiogenesis in the bone marrow of children with acute lymphoblastic leukemia. Am. J. Pathol., *150:* 815–821, 1997.
5. Hussong, J. W., Rodgers, G. M., and Shami, P. J. Evidence of increased angiogenesis in patients with acute myeloid leukemia. Blood, *95:* 309–313, 2000.
6. Aguayo, A., Kantarjian, H., Manshouri, T., Gidel, C., Estey, E., Thomas, D., Koller, C., Estrov, Z., O'Brien, S., Keating, M., Freireich, E., and Albitar, M. Angiogenesis in acute and chronic leukemias and myelodysplastic syndromes. Blood, *96:* 2240–2245, 2000.
7. Kini, A. R., Kay, N. E., and Peterson, L. C. Increased bone marrow angiogenesis in B cell chronic lymphocytic leukemia. Leukemia, *14:* 1414–1418, 2000.
8. Yang, C., Chang, J., Gorospe, M., and Passaniti, A. Protein tyrosine phosphatase regulation of endothelial cell apoptosis and differentiation. Cell Growth Differ., *7:* 161–171, 1996.
9. Dvorak, H. F., Brown, L. F., Detmar, M., and Dvorak, A. M. Vascular permeability factor/vascular endothelial growth factor, microvascular hyperpermeability, and angiogenesis. Am. J. Pathol., *146:* 1029–1039, 1995.
10. Browder, T., Folkman, J., and Pirie-Shepherd, S. The hemostatic system as a regulator of angiogenesis. J. Biol. Chem., *275:* 1521–1524, 2000.
11. Grant, D. S., and Kleinman, H. K. Regulation of capillary formation by laminin and other components of the extracellular matrix. EXS., *79:* 317–333, 1997.
12. Rabbani, S. A. Metalloproteases and urokinase in angiogenesis and tumor progression. In Vivo, *12:* 135–142, 1998.
13. Haas, T. L., and Madri, J. A. Extracellular matrix-driven matrix metalloproteinase production in endothelial cells: implications for angiogenesis. Trends Cardiovasc. Med., *9:* 70–77, 1999.
14. Streuli, C. Extracellular matrix remodeling and cellular differentiation. Curr. Opin. Cell Biol., *11:* 634–640, 1999.
15. Naito, S., Shimizu, K., Nakashima, M., Nakayama, T., Ito, T., Ito, M., Yamashita, S., and Sekine, I. Overexpression of Ets-1 transcription factor in angiosarcoma of the skin. Pathol. Res. Pract., *196:* 103–109, 2000.
16. Watabe, T., Yoshida, K., Shindoh, M., Kaya, M., Fujikawa, K., Sato, H., Seiki, M., Ishii, S., and Fujinaga, K. The Ets-1 and Ets-2 transcription factors activate the promoters for invasion-associated urokinase and collagenase genes in response to epidermal growth factor. Int. J. Cancer, *77:* 128–137, 1998.
17. Sato, Y. Transcription factor ETS-1 as a molecular target for angiogenesis inhibition. Hum. Cell., *11:* 207–214, 1998.
18. Tanaka, K., Oda, N., Iwasaka, C., Abe, M., and Sato, Y. Induction of Ets-1 in endothelial cells during reendothelialization after denuding injury. J. Cell. Physiol., *176:* 235–244, 1999.
19. Lyden, D., Young, A. Z., Zagzag, D., Yan, W., Gerald, W., O'Reilly, R., Bader, B. L., Hynes, R. O., Zhuang, Y., Manova, K., and Benezra, R. Id1 and Id3 are required for neurogenesis, angiogenesis and vascularization of tumour xenografts. Nature (Lond.), *401:* 670–677, 1999.
20. Bi, W., Drake, C. J., and Schwarz, J. J. The transcription factor MEF2C-null mouse exhibits complex vascular malformations and reduced cardiac expression of angiopoietin 1 and VEGF. Dev. Biol. *211:* 255–267, 1999.
21. Drake, C. J., Hungerford, J. E., and Little, C. D. Morphogenesis of the first blood vessels. Ann. N. Y. Acad. Sci., *857:* 155–179, 1998.
22. Xiong, J. W., Leahy, A., Lee, H. H., and Stuhlmann, H. Vezf1: A Zn finger transcription factor restricted to endothelial cells and their precursors. Dev. Biol., *206:* 123–141, 1999.
23. Ryuto, M., Ono, M., Izumi, H., Yoshida, S., Weich, H. A., Kohno, K., and Kuwano, M. Induction of vascular endothelial growth factor by tumor necrosis factor α in human glioma cells. Possible roles of SP-1. J. Biol. Chem., *271:* 28220–28228, 1996.
24. Navab, M., Fogelman, A. M., Berliner, J. A., Territo, M. C., Demer, L. L., Frank, J. S., Watson, A. D., Edwards, P. A., and Lusis, A. J. Pathogenesis of atherosclerosis. Am. J. Cardiol., *76:* 18C–23C, 1995.

25. Kim-Schulze, S., Lowe, W. L., Jr., and Schnaper, H. W. Estrogen stimulates delayed mitogen-activated protein kinase activity in human endothelial cells via an autocrine loop that involves basic fibroblast growth factor. Circulation, *98:* 413–421, 1998.
26. Oike, Y., Takakura, N., Hata, A., Kaname, T., Akizuki, M., Yamaguchi, Y., Yasue, H., Araki, K., Yamamura, K., and Suda, T. Mice homozygous for a truncated form of CREB-binding protein exhibit defects in hematopoiesis and vasculo-angiogenesis. Blood, *93:* 2771–2779, 1999.
27. Semenza, G. L. Regulation of mammalian O2 homeostasis by hypoxia-inducible factor 1. Annu. Rev. Cell Dev. Biol., *15:* 551–578, 1999.
28. Westendorf, J. J., and Hiebert, S. W. Mammalian runt-domain proteins and their roles in hematopoiesis, osteogenesis, and leukemia. J. Cell. Biochem. *3433* (Suppl.)*:*, 51–58, 1999.
29. Wang, Q., Stacy, T., Binder, M., Marin-Padilla, M., Sharpe, A., and Speck, N. Disruption of the *Cbfa2* gene causes necrosis and hemorrhaging in the central nervous system and blocks definitive hematopoiesis. Proc. Natl. Acad. Sci. USA, 3444–3449, 1996.
30. Takakura, N., Watanabe, T., Suenobu, S., Yamada, Y., Noda, T., Ito, Y., Satake, M., and Suda, T. A role for hematopoietic stem cells in promoting angiogenesis. Cell, *102:* 199–209, 2000.
31. Ducy, P., Zhang, R., Geoffroy, V., Ridall, A. L., and Karsenty, G. Osf2/RUNX2: a transcriptional activator of osteoblast differentiation. Cell, *89:* 747–754, 1997.
32. Banerjee, C., McCabe, L. R., Choi, J. Y., Hiebert, S. W., Stein, J. L., Stein, G. S., and Lian, J. B. Runt homology domain protein in osteoblast differentiation: AML3/CBFA1 is a major component of a bone-specific complex. J. Cell. Biochem., *66:* 1–8, 1997.
33. Akiyama, H., Kanno, T., Ito, H., Terry, A., Neil, J., Ito, Y., and Nakamura, T. Positive and negative regulation of chondrogenesis by splice variants of PEBP2αA/CBFα1 in clonal mouse EC cells, ATDC5. J. Cell. Physiol., *181:* 169–178, 1999.
34. Namba, K., Abe, M., Saito, S., Satake, M., Ohmoto, T., Watanabe, T., and Sato, Y. Indispensable role of the transcription factor PEBP2/CBF in angiogenic activity of a murine endothelial cell MSS31. Oncogene, *19:* 106–114, 2000.
35. Kleinman, H. K., McGarvey, M. L., Hassell, J. R., Star, V. L., Cannon, F. B., Laurie, G. W., and Martin, G. R. Basement membrane complexes with biological activity. Biochemistry, *25:* 312–318, 1986.
36. Lehr, J. E., and Pienta, K. J. Preferential adhesion of prostate cancer cells to a human bone marrow endothelial cell line. J. Natl. Cancer Inst., *90:* 118–123, 1998.
37. Ades, E. W., Candal, F. J., Swerlick, R. A., George, V. G., Summers, S., Bosse, D. C., and Lawley, T. J. HMEC-1: establishment of an immortalized human microvascular endothelial cell line. J. Investig. Dermatol., *99:* 683–690, 1992.
38. Sasaki, C. Y., and Passaniti, A. Identification of anti-invasive but noncytotoxic chemotherapeutic agents using the tetrazolium dye MTT to quantitate viable cells in Matrigel. Biotechniques, *24:* 1038–1043, 1998.
39. Sun, L., Margolis, F. L., Shipley, M. T., and Lidow, M. S. Identification of a long variant of mRNA encoding the NR3 subunit of the NMDA receptor: its regional distribution and developmental expression in the rat brain. FEBS Lett., *441:* 392–396, 1998.
40. Xiao, G., Wang, D., Benson, M. D., Karsenty, G., and Franceschi, R. T. Role of the α2-integrin in osteoblast-specific gene expression and activation of the Osf2 transcription factor. J. Biol. Chem., *273:* 32988–32994, 1998.
41. Smith, L. E., Shen, W., Perruzzi, C., Soker, S., Kinose, F., Xu, X., Robinson, G., Driver, S., Bischoff, J., Zhang, B., Schaeffer, J. M., and Senger, D. R. Regulation of vascular endothelial growth factor-dependent retinal neovascularization by insulin-like growth factor-1 receptor. Nat. Med., *5:* 1390–1395, 1999.
42. Shi, Q., Rafii, S., Wu, M. H., Wijelath, E. S., Yu, C., Ishida, A., Fujita, Y., Kothari, S., Mohle, R., Sauvage, L. R., Moore, M. A., Storb, R. F., and Hammond, W. P. Evidence for circulating bone marrow-derived endothelial cells. Blood, *92:* 362–367, 1998.
43. Garlanda, C., and Dejana, E. Heterogeneity of endothelial cells. Specific markers. Arterioscler. Thromb. Vasc. Biol., *17:* 1193–1202, 1997.
44. McCarthy, S. A., Kuzu, I., Gatter, K. C., and Bicknell, R. Heterogeneity of the endothelial cell and its role in organ preference of tumor metastasis. Trends Pharmacol. Sci., *12:* 462–467, 1991.
45. Singh, D., Joshi, D. D., Hameed, M., Qian, J., Gascon, P., Maloof, P. B., Mosenthal, A., and Rameshwar, P. Increased expression of preprotachykinin-I and neurokinin receptors in human breast cancer cells: implications for bone marrow metastasis. Proc. Natl. Acad. Sci. USA, *97:* 388–393, 2000.
46. Gehling, U. M., Ergun, S., Schumacher, U., Wagener, C., Pantel, K., Otte, M., Schuch, G., Schafhausen, P., Mende, T., Kilic, N., Kluge, K., Schafer, B., Hossfeld, D. K., and Fiedler, W. *In vitro* differentiation of endothelial cells from AC133-positive progenitor cells. Blood, *95:* 3106–3112, 2000.
47. Dankbar, B., Padro, T., Leo, R., Feldmann, B., Kropff, M., Mesters, R. M., Serve, H., Berdel, W. E., and Kienast, J. Vascular endothelial growth factor and interleukin-6 in paracrine tumor-stromal cell interactions in multiple myeloma. Blood, *95:* 2630–2636, 2000.
48. Vacca, A., Ribatti, D., Presta, M., Minischetti, M., Iurlaro, M., Ria, R., Albini, A., Bussolino, F., and Dammacco, F. Bone marrow neovascularization, plasma cell angiogenic potential, and matrix metalloproteinase-2 secretion parallel progression of human multiple myeloma. Blood, *93:* 3064–3073, 1999.
49. Baker, J., Liu, J. P., Robertson, E. J., and Efstratiadis, A. Role of insulin-like growth factors in embryonic and postnatal growth. Cell, *75:* 73–82, 1993.
50. Xiao, G., Jiang, D., Thomas, P., Benson, M. D., Guan, K., Karsenty, G., and Franceschi, R. T. MAPK pathways activate and phosphorylate the osteoblast-specific transcription factor, RUNX2. J. Biol. Chem., *275:* 4453–4459, 2000.
51. Morino, N., Mimura, T., Hamasaki, K., Tobe, K., Ueki, K., Kikuchi, K., Takehara, K., Kadowaki, T., Yazaki, Y., and Nojima, Y. Matrix/integrin interaction activates the mitogen-activated protein kinase, p44erk-1 and p42erk-2. J. Biol. Chem., *270:* 269–273, 1995.
52. Senger, D. R., Ledbetter, S. R., Claffey, K. P., Papadopoulos-Sergiou, A., Peruzzi, C. A., and Detmar, M. Stimulation of endothelial cell migration by vascular permeability factor/vascular endothelial growth factor through cooperative mechanisms involving the $\alpha v\beta 3$ integrin, osteopontin, and thrombin. Am. J. Pathol., *149:* 293–305, 1996.
53. Stetler-Stevenson, W. G. Matrix metalloproteinases in angiogenesis: a moving target for therapeutic intervention. J. Clin. Investig., *103:* 1237–1241, 1999.
54. Nagase, H., and Woessner, J. F., Jr. Matrix metalloproteinases. J. Biol. Chem., *274:* 21491–21494, 1999.
55. Ito, Y. Molecular basis of tissue-specific gene expression mediated by the runt domain transcription factor PEBP2/CBF. Genes Cells. *4:* 685–696, 1999.

Runt-related Gene 2 in Endothelial Cells: Inducible Expression and Specific Regulation of Cell Migration and Invasion

Lixin Sun, Michele Vitolo and Antonino Passaniti

Cancer Res 2001;61:4994-5001.